Photochemical & Photobiological Sciences

Cite this: DOI: 10.1039/c2pp25039j

www.rsc.org/pps

PAPER

Photophysical study of 2-(4′-*N*,*N*-dimethylaminophenyl)oxazolo[4,5-*b*]-pyridine in different solvents and at various pH†

Anasuya Mishra and G. Krishnamoorthy*

Received 24th February 2012, Accepted 6th May 2012
DOI: 10.1039/c2pp25039j

The spectral characteristics of 2-(4′-*N*,*N*-dimethylaminophenyl)oxazolo[4,5-*b*]pyridine (DMAPOP) have been investigated in solvents of different polarity and hydrogen bonding capacity. Unlike its imidazole analogue, DMAPOP emits single emission in both aprotic and protic solvents and the hydrogen-bond induced TICT emission is not observed in any protic solvents. The solvent effect on both absorption and the emission spectral data are analyzed by multiple parametric regression analysis. The prototropic studies reveal that two kinds of monocations are formed by protonation of pyridine nitrogen (MC1) and the dimethylamino nitrogen (MC3) in both ground and excited states. However three kinds of dications are formed by protonation of pyridine and oxazole nitrogens (DC1), pyridine and dimethylamino nitrogens (DC2), and dimethylamino and oxazole nitrogens (DC3).

1. Introduction

Oxazoles are an important class of molecules of the azole family and are known for their biological activity. For example, oxazole derivatives are used as anti-inflammatories, analgesics, anti-pyretics and antagonists.[1–4] Owing to their wide applications as fluorescent sensors, fluorescent brighteners, and laser diodes, the study on the optical characteristics of oxazoles has gained interest.[5–8]

We have recently studied the fluorescence characteristics of 2-(4′-*N*,*N*-dimethylamino)imidazo[4,5-*b*]pyridine (DMAPIP, Chart 1) and found that DMAPIP exhibits single emission in aprotic solvents and dual emission in polar protic solvents (except water).[9] The dual emission in protic solvent is due to formation of a twisted intramolecular charge transfer (TICT) state. In water the TICT emission was quenched completely due to an increase in the nonradiative rate by greater stabilization of the TICT state. Our studies suggested that the hydrogen bonding of the protic solvents with the pyridine nitrogen plays a crucial role in the formation of TICT state in DMAPIP.[9–11] Further, we have shown that DMAPIP can be used as a probe to investigate micro-heterogeneous systems.[12,13] Therefore it is interesting to study the effect of oxygen substitution on the spectral characteristics and such a study may be useful in understanding the protic solvent-induced TICT emission observed in DMAPIP. Recently Mac *et al.* studied the fluorescence properties of several oxazolo-[4,5-*b*]pyridines including 2-(4′-*N*,*N*-diethylaminophenyl)oxazolo-[4,5-*b*]pyridine (DEAPOP, Chart 1), and found that the dyes possess charge transfer character in the ground and the excited states. However, they did not observe dual emission from any molecule including DEAPOP. But their studies are restricted to nonpolar and polar aprotic solvents.[14] Mac *et al.* also studied the prototropic equilibria of DEAPOP and found two absorption bands due to formation of two kinds of monocations. On the other hand they reported that only one fluorescence spectrum corresponds to one of the monocations.

Thus, we have synthesized and studied the spectral characteristics of 2-(4′-*N*,*N*-dimethylaminophenyl)oxazolo[4,5-*b*]pyridine (DMAPOP) in solvents of different polarity and hydrogen-bonding capacity and at different pH in aqueous media. The main objectives of the studies are to investigate (i) the effect of protic solvents on the fluorescence characteristics of DMAPOP and (ii) to understand the excited state prototropic equilibria of DMAPOP.

2. Materials and methods

DMAPOP was synthesized by refluxing equimolar mixture of 2-amino-3-hydroxypyridine and 4-(*N*,*N*-dimethylamino)benzoic acid in $POCl_3$ for 8 hours by following the procedure reported for similar compounds.[15] The reaction mixture was cooled to room temperature and poured into ice cold water. It was neutralized by concentrated sodium hydroxide solution and the precipitate was collected. The compound was purified by column chromatography. The compound was confirmed by ^{1}H NMR spectroscopy and mass spectrometry as follows. ^{1}H NMR (400 MHz, CD_3Cl, ppm) δ 8.46 (d, J = 5 Hz, 1H); 8.14 (d, J = 8 Hz, 2H); 7.86 (d, J = 8 Hz, 1H); 7.16 (dd, (J = 5.2, 8) Hz, 1H); 6.75 (d, J = 9.2 Hz, 2H); 3.07 (s, 6H). From HRMS the molecular mass (M + 1) was found to be m/z: 240.1211.

HPLC grade solvents were used for solvent study and millipore water was used for the preparation of aqueous solutions. Aqueous solutions in the pH range 3–11 were prepared by

Department of Chemistry, Indian Institute of Technology, Guwahati, Guwahati 781039, India. E-mail: gkrishna@iitg.ernet.in
† Dedicated to Prof. S. K. Dogra on the occasion of his 70th birthday.

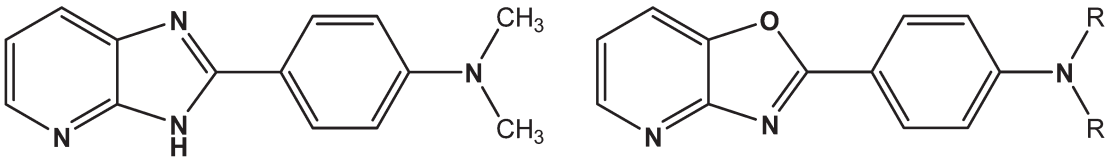

Chart 1 Structures of DMAPOP and related molecules.

mixing appropriate amounts of dilute solutions of NaOH and H_3PO_4. Hammett's acidity scale (H_0) was used in preparing solutions of pH < 1.0.[16] The pH of different solutions were measured using Jenway (model No 3510) pH meter. The pH meter was calibrated by using three different standard buffer solutions (pH 4, pH 7 and pH 10) within a range of ±0.02 pH units before any measurement. The solvents were transparent in the spectral region of interest and were used as received. A Varian Cary 100 UV-visible spectrophotometer and a Jobin Yvon Spex Fluoromax 4 instrument were used to collect absorption and fluorescence spectra, respectively. The fluorescence quantum yields were measured at λ_{exc} 350 nm with respect to quinine sulfate in 1 N sulfuric acid ($\Phi_f = 0.55$).[17] For fluorescence measurements the absorbance of the solutions is kept at ~0.1 at the absorption maxima. Lifetime was measured with an Edinburgh life spec II instrument, where the fluorescence lifetimes were determined from time-resolved intensity decay by the method of time-correlated single-photon counting using a picosecond 375 nm laser diode as light source. The data were analyzed by the reconvolution method using the software provided by Edinburgh instruments.

As determination of the concentration ratio [acidic form]/[basic form] is difficult due to the complicated nature of the prototropic equilibria, calculating the accurate pK_a value for the prototropic equilibria of DMAPOP is not feasible. However, the pK_a value for the neutral-monocation equilibrium was estimated from the plot of absorbance against pH. Absorbance at 342 nm where the absorbance of monocation(s) is least is used to estimate the pK_a value for the neutral-monocation equilibrium.

3. Results and discussion

3.1. Solvent effect on absorption and fluorescence spectra

The absorption and the fluorescence spectral data of DMAPOP are compiled in Table 1. Fig. 1 depicts the fluorescence spectra in different solvents. The fluorescence spectrum is structured in nonpolar solvents. Upon increasing the polarity and the hydrogen bonding capacity of the solvent the fluorescence is blurred with a bathochromic shift. The bathochromic shift is more pronounced in DMAPOP than the corresponding imidazole derivative.[9] For example, from cyclohexane to methanol, a 22 nm shift in the absorption spectra and a 43 nm shift in the fluorescence spectra are observed for DMAPOP (Table 1). On the other hand the bathochromic shifts are only 14 nm and 35 nm respectively in the absorption and fluorescence spectra of DMAPIP.[9] In polar media, a red shift is observed for the electronic transition of the type π–π* due to greater stabilization of the ππ* state by the

Table 1 Longest wavelength absorption maxima (λ^{ab}_{max}, nm), fluorescence emission maxima (λ^{ab}_{max} , nm), Stokes shift (ν_{SS}, cm^{-1}), fluorescence quantum yield (Φ_f), life time (τ, ns), radiative rate constant (k_r, s^{-1}) and nonradiative rate constant (k_{nr}, s^{-1}) of DMAPOP in different solvents

Solvents	λ^{ab}_{max}	λ^{em}_{max}	$\bar{\nu}_{SS}$	Φ_f	τ	k_r (10^8)	k_{nr} (10^8)
Hexane	341, 358 (sh)	364, 384, 407 (sh)	3284	0.96	1.2	8.1	0.4
Cyclohexane	343, 360 (sh)	366, 386, 408 (sh)	3248	0.94	1.2	7.8	0.5
Dioxane	354	404	3496	0.99	1.3	7.6	0.01
Ether	352	397	3220	0.88	1.3	7.0	1.0
DMF	362	424	4039	0.88	1.4	6.4	0.9
Acetonitrile	358	418	4010	0.86	1.5	5.6	0.9
Methanol	365	429	4087	0.60	1.1	5.2	3.6
Ethanol	364	427	4053	0.83	1.5	5.6	1.1
1-Propanol	366	425	3793	0.94	1.5	6.1	0.4
2-Propanol	362	421	3871	0.99	1.5	6.4	0.1
Butanol	364	420	3663	0.94	1.5	6.2	0.4
Glycol	373	438	3979	0.51	1.0	4.9	4.7
Glycerol	376	442	3971	0.90	1.5	6.2	0.7
Water	365	448	5076				

increase in the charge transfer nature. Therefore it is clear that the substitution of electronegative oxygen increases the charge flow from the dimethylamino group to oxazolopyridine ring. Further the absorption spectrum of DMAPIP in water was blue shifted with respect to that in methanol owing to the greater hydrogen bonding of water over methanol with the dimethylamino nitrogen. But no such hypsochromic effect was observed in the absorption spectral maxima of DMAPOP, substantiating the increase in charge flow from the dimethylamino group to the oxazalopyridine ring.

Multiple linear regression analysis by using Abraham *et al.*'s solvatochromic approach is performed to identify the different modes of solvation determining the absorption and emission energies.[18] The equations obtained by solvatochromic multiparametric method are

$$E(\mathrm{A}) = 29158 - 1131\pi^* - 524\alpha - 867\beta$$

$$E(\mathrm{F}) = 25970 - 2192\pi^* - 1029\alpha - 498\beta$$

where E(A) and E(F) are absorption and fluorescence band maxima in cm^{-1}, respectively. Good correlations are found for E(A) and E(F) with Taft *et al.*'s π^*, α and β values, where π^* denotes the dielectric effects of solvents, and α and β are the hydrogen-bond donor ability and the hydrogen-bond acceptor ability of the solvents, respectively.[19] The regression value

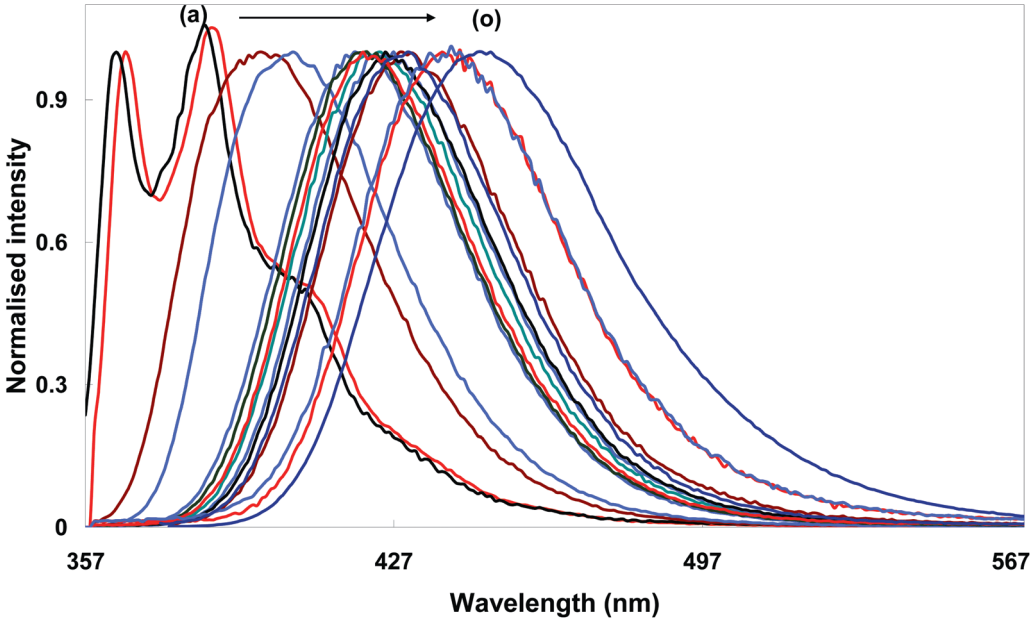

Fig. 1 Normalized fluorescence spectra (λ_{ex} = 350 nm) of DMAPOP in (a) hexane, (b) cyclohexane, (c) ether, (d) dioxane, (e) acetonitrile, (f) 2-propanol, (g) butanol, (h) DMF, (i) ethanol, (j) 1-propanol, (k) DMSO, (l) methanol, (m) ethylene glycol, (n) glycerol, (o) water.

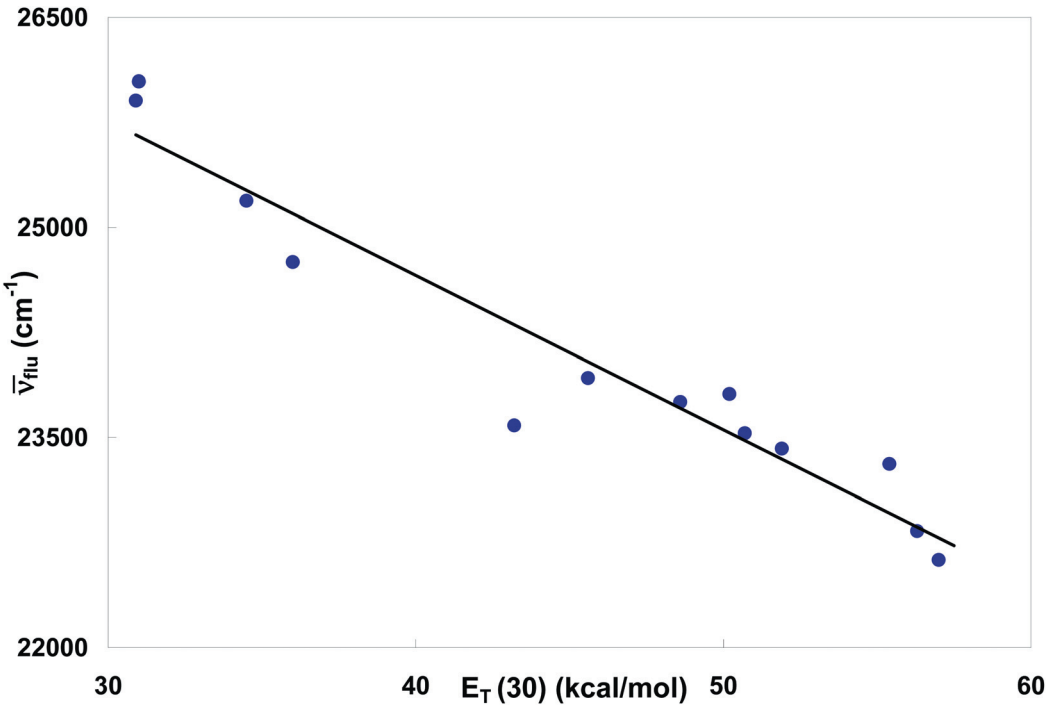

Fig. 2 Plot of $\bar{\nu}_{flu}$ *versus* $E_T(30)$ parameters.

obtained for absorption and fluorescence data were 0.97 and 0.99 respectively. E_0 values obtained are also in good agreement with the experimental values in nonpolar solvent. Negative values of π^*, α and β indicate all the three parameters contribute to the stabilization of both the ground state and the excited state of the molecule. A good linear variation is also obtained between the fluorescence maxima and the $E_T(30)$ values[20] (Fig. 2).

The Lippert–Mataga plot[21] was constructed (Fig. 3) by using the relation

$$\bar{\nu}_{SS} = [2(\mu_e - \mu_g)/hca^3]\Delta f + \nu_{SS}^{o}$$

where $\bar{\nu}_{SS}$ is the Stokes shift, the superscript "o" indicates the absence of solvent, μ_g and μ_e are dipole moments in the ground state and excited state respectively, a is the Onsager cavity

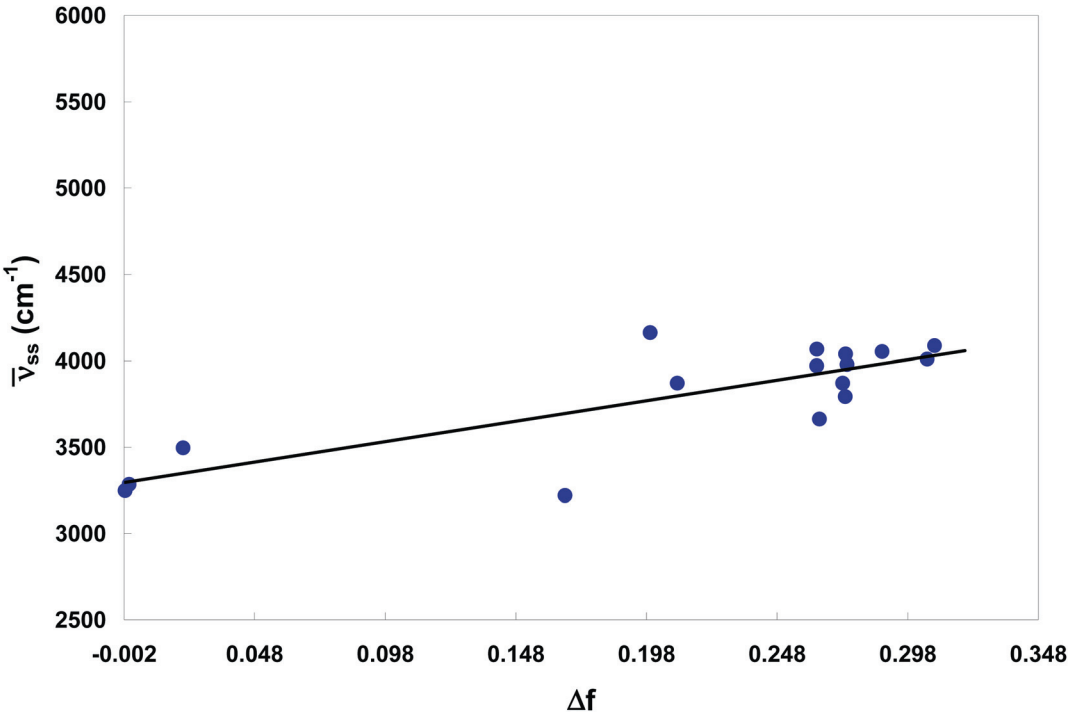

Fig. 3 Lippert–Mataga plot for DMAPOP.

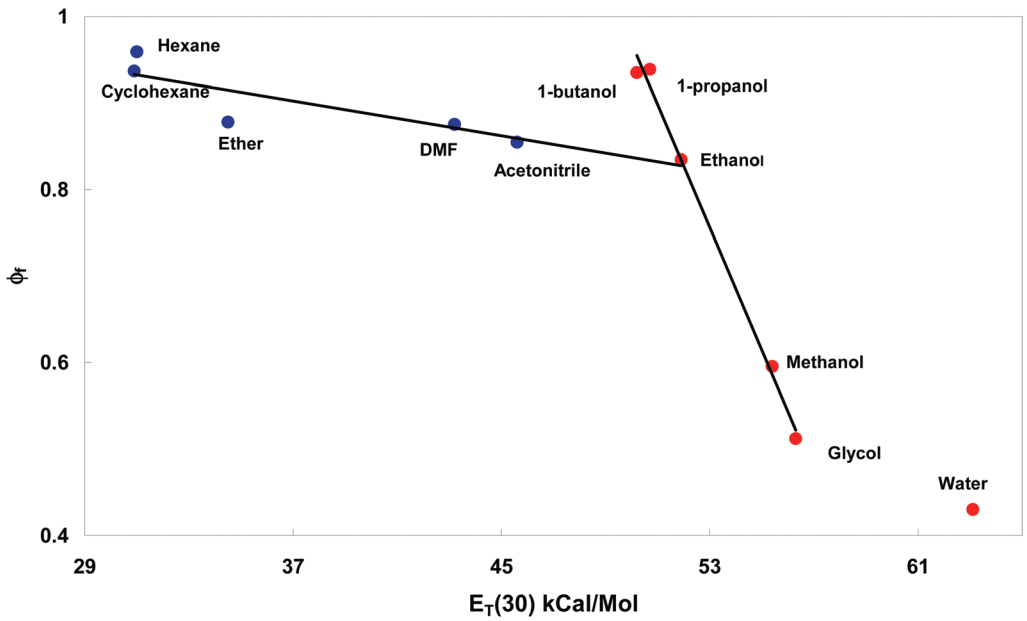

Fig. 4 Plot of variation of fluorescence quantum yield of DMAPOP as a function of solvent polarity.

radius. The orientation polarizability Δf is defined as

$$\Delta f = [(\varepsilon - 1)/(2\varepsilon + 1)] - [(n^2 - 1)/(2n^2 + 1)]$$

where ε and n are solvent dielectric constant and refractive index, respectively. The geometrical optimization of DMAPOP was done by DFT method using Gaussian 03 software to calculate the μ_g.[22] Using 5.9 D, the μ_g value obtained from the DFT calculation and the slope of Lippert–Mataga plot the value of μ_e is calculated. The μ_e value thus obtained is 10.6 D. The value is a little higher than 10.4 D reported for DEAPOP.[14]

Fluorescence quantum yields of DMAPOP measured in different solvents are presented in Table 1 and the variation of quantum yield with solvent polarity parameter $E_T(30)$ is shown in Fig. 4. It is clear from the plot that fluorescence quantum yield of DMAPOP decreases with increasing polarity of the

solvents and the decrease is less prominent in nonpolar and polar aprotic solvents. But in the case of polar protic solvents the change is much more prominent with a steep slope. The significant decrease of quantum yield observed upon increasing the protic nature of the medium suggested the differential contribution of charge transfer and hydrogen bonding interactions.[23] Owing to greater viscosity of the solvent DMAPOP has higher quantum yield in glycerol.

Radiative (k_r) and nonradiative (k_{nr}) rate constants are calculated from fluorescence quantum yields and lifetime values of DMAPOP in different solvents to understand the effect of solvation on the dynamics of the excited state. A typical set of k_r and k_{nr} values are tabulated (Table 1). The logarithm of (k_r/k_{nr}) of DMAPOP is plotted against the solvent polarity parameter $E_T(30)$ (Fig. 5). Two different straight lines are obtained, one for aprotic solvents and the other for protic solvents. In both the cases, upon increasing the polarity the logarithm ratio of radiative to nonradiative rate decreases but a steeper slope is obtained in the case of protic solvents. It indicates that the radiative and nonradiative rates are more sensitive toward protic solvents. It may be that the hydrogen bonding interaction in polar protic environments enhances the stabilization of the S_1 state of DMAPOP as a result the nonradiative relaxation rate increases.[23]

The striking difference between DMAPOP and its imidazole analogue DMAPIP is the absence of longer wavelength emission in protic solvents. The single exponential decays in protic solvents further substantiates the non-dual fluorescence nature of DMAPOP. Our earlier studies indicate that the hydrogen bonding of the solvent with pyridine nitrogen plays a major role in the formation of TICT state in DMAPIP.[9] The present study suggests that the 'NH' group of the imidazole nitrogen may also play a crucial role in the formation of the TICT state in DMAPIP. One possibility that comes to mind is proton transfer from the imidazole 'NH' nitrogen to the pyridine nitrogen coupled with charge transfer. Yoon *et al.* proposed such a model to explain the formation of TICT emission in 4-(*N*,*N*-dimethylamino)salicylic acid in nonpolar solvent.[24] Further investigations on dual fluorescence of DMAPIP are in progress.

3.2 Prototropic equilibria

Different possible cations that can be formed by the protonation of the basic nitrogens in DMAPOP are presented in Scheme 1.

Upon decreasing the pH two new bands appear in the absorption spectra of DMAPOP with two quasi-isosbestic points at 324 nm and 395 nm (Fig. 6). This indicates the formation of two kinds of monocations. The emission spectra are quite complicated. Excitation at 324 nm, the isosbestic point, resulted in two-band systems with a quasi-isoemissive point at 412 nm (Fig. 7a). This suggests equilibrium between the neutral form and the monocation. On the other hand the fluorescence spectrum corresponding to the neutral molecule is predominantly observed when excited at the red-side isosbestic point (λ_{exc} = 395 nm, not shown). The intensity of the neutral fluorescence band decreases with increase in acid concentration. However excitation at the red absorption band (λ_{exc} = 430 nm) produces an additional weak emission at 560 nm (Fig. 7b). With decrease in pH the intensity of the 560 nm emission also increases at the cost of the neutral emission. The spectral data are compiled in Table 2. This clearly establishes that two kinds of monocations are present in both ground and excited states. Protonation of the dimethylamino nitrogen leads to a blue shift, and protonation of the ring nitrogens leads to a red shift and the shift is more in case of pyridine nitrogen than imidazole nitrogen.[25–27] Therefore the blue-shifted band at 308 nm in the absorption spectrum and the corresponding fluorescence spectrum at 350 nm can be assigned to the monocation formed by the protonation of dimethylamino nitrogen *i.e.* MC3 (Scheme 1). Based on the following facts the red-shifted absorption and the fluorescence spectra are assigned

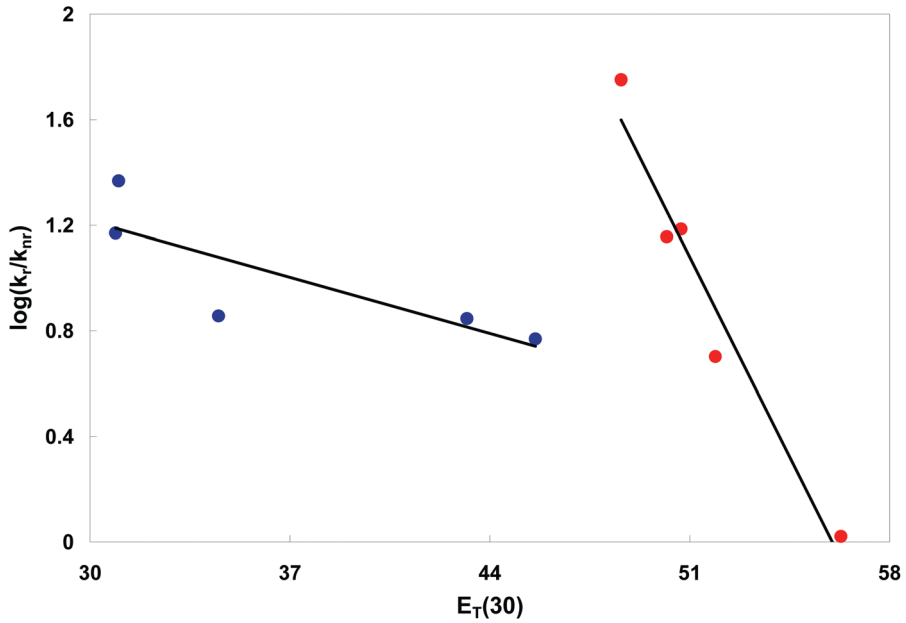

Fig. 5 Plot of $\log(k_r/k_{nr})$ *versus* $E_T(30)$ in various solvents.

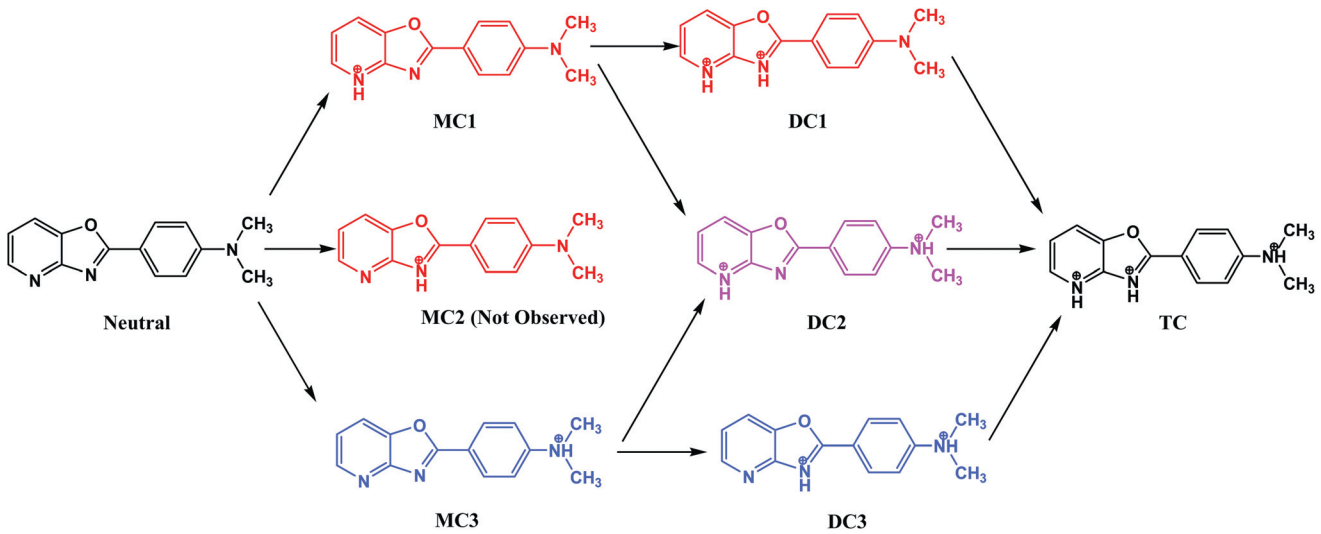

Scheme 1 Prototropic reactions of DMAPOP.

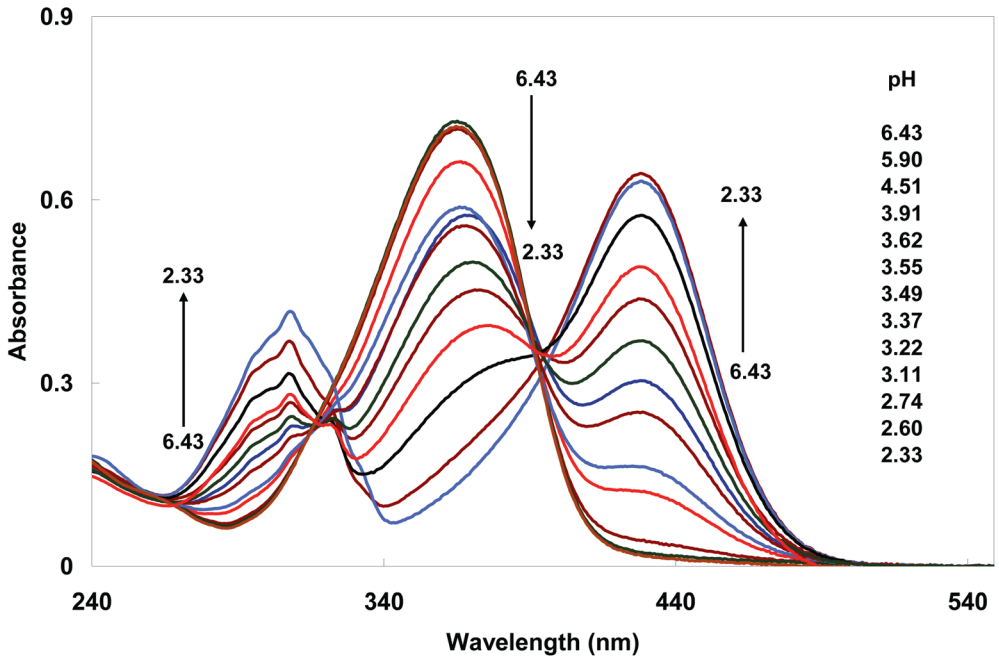

Fig. 6 Absorption spectra of DMAPOP for neutral-monocation equilibrium in water.

to the monocation formed by the protonation of the pyridine nitrogen (MC1) rather than the oxazole nitrogen (MC2). (i) Due to higher charge transfer character of MC1 than MC2, a large Stokes shift is expected in the fluorescence spectrum of MC1 than MC2. The observed Stokes shift (5500 cm^{-1}) for the monocation is closer to that of MC1 of DMAPIP rather than MC2 of DMAPIP and the Stokes shift is also much higher than that obtained for the monocation formed by the protonation of imidazole nitrogen (1850 cm^{-1}) in 2-(4′-*N*,*N*-dimethylaminophenyl)benzoxazole (Chart 2).[13,27–29] (ii) The pK_a value (3.35) obtained for DMAPOP is higher than that of oxazole nitrogen protonation (2.35) in 2-(4′-*N*,*N*-dimethylaminophenyl)benzoxazole.[28] This is consistent with the fact that pyridine nitrogen protonation has a higher pK_a value for the neutral-monocation equilibrium than that of imidazole nitrogen protonation,[9,25,26,28] although we observe both MC1 and MC2 in the excited state.

The results of neutral-monocation equilibrium of DMAPOP and other related molecules (Chart 2) from the literature are summarized in Table 3. In 2-(4′-*N*,*N*-dimethylaminophenyl)-benzimidazole, due to an increase in charge flow from the dimethylamino nitrogen to the imidazole nitrogen, protonation predominantly occurs at the imidazole nitrogen and a small

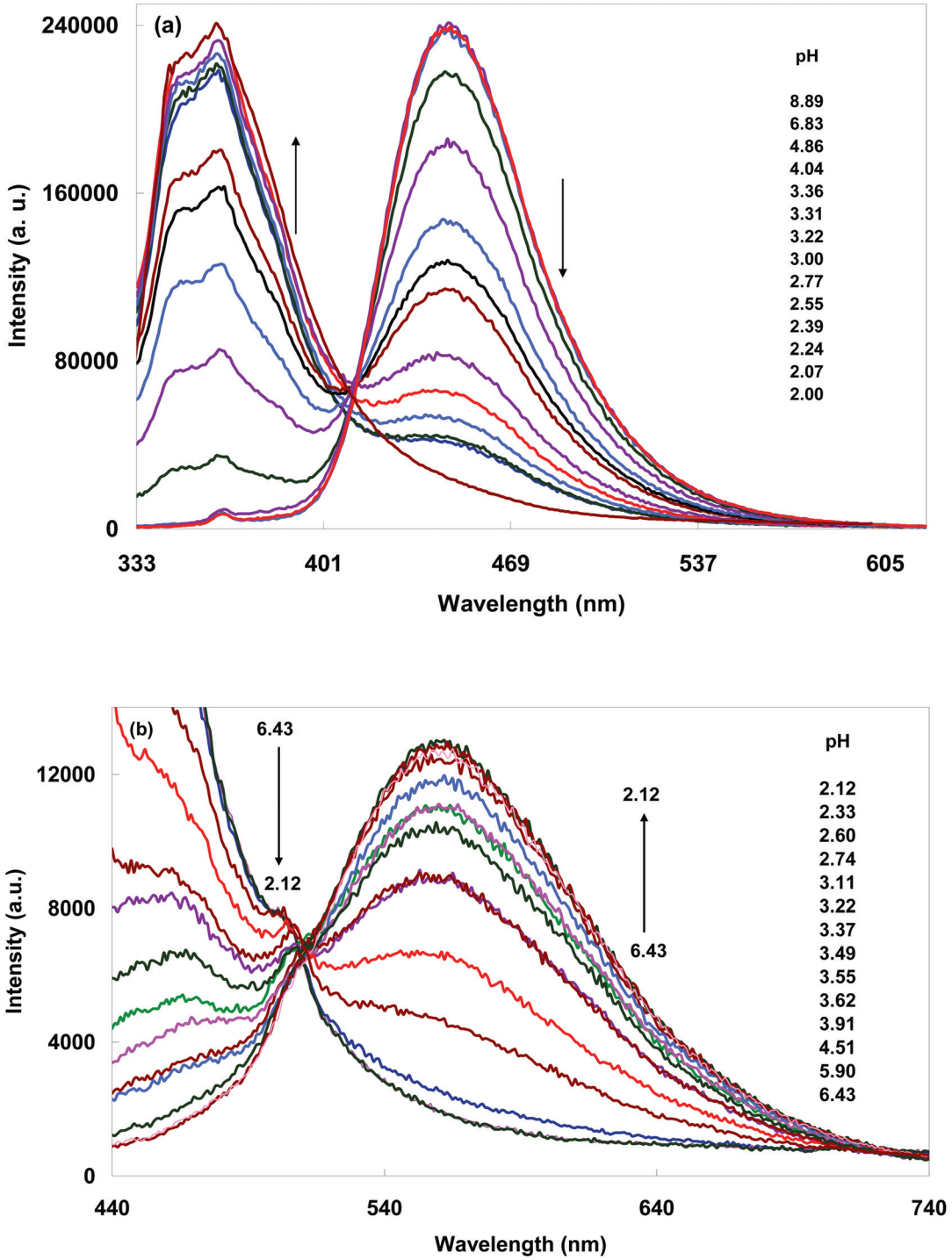

Fig. 7 Emission spectra of DMAPOP by (a) λ_{exc} = 324 nm, (b) λ_{exc} = 430 at different pH (the shoulder peak at 506 nm is due to water Raman emission).

amount of protonation occurs at the dimethylamino nitrogen.[29] When the >NH group is replaced by oxygen, it reduces the charge density on the oxazole nitrogen in 2-(4′-*N*,*N*-dimethylaminophenyl)benzoxazole and protonation at the oxazole nitrogen decreases and that at the dimethylamino increases.[28] On the other hand, when nitrogen is substituted in benzene ring (DMAPIP) no protonation occurs at dimethylamino nitrogen and it occurs at the imidazole nitrogen with a small amount at the pyridine nitrogen. In DMAPOP the pyridine nitrogen is substituted in the benzene ring and the >NH group is replaced by oxygen, the formation of MC2 (*i.e.* protonation at imidazole nitrogen) is completely terminated and the protonation at pyridine nitrogen dominates over that at dimethylamino nitrogen (Scheme 1). It appears that substitution of more electronegative oxygen decreases the electron density on the imidazole nitrogens. This is substantiated by the lower pK_a values for the

Table 2 Absorption band maxima (λ^{ab}_{max}, nm), excitation band maxima (λ^{exc}_{max}, nm) and emission band maxima (λ^{em}_{max}, nm) for different prototropic species in water

Species	λ^{ab}_{max}	λ^{exc}_{max}	λ^{em}_{max}
Neutral	365	366	447
MC1	428	428	560
MC3	306	308, 321	350, 365
DC1		595	700
DC2		360	480
DC3	317, 331	319, 332	360, 375
TC	325	327	354, 370, 384

Table 3 pK_a values of neutral-monocation of different molecules along with the site of protonation (see Chart 2 for monocation labelling)

Molecule	pK_a	Monocation formed
2-(4′-*N*,*N*-Dimethylaminophenyl)-benzimidazole[a]	5.60	MC2 ≫ MC3
2-(4′-*N*,*N*-Dimethylaminophenyl)-benzoxazole[b]	2.35	MC3 > MC2
DMAPIP[c]	5.40	MC2 > MC1
DMAPOP	3.35	MC1 > MC3

[a] Ref. 26. [b] Ref. 28. [c] Ref. 9.

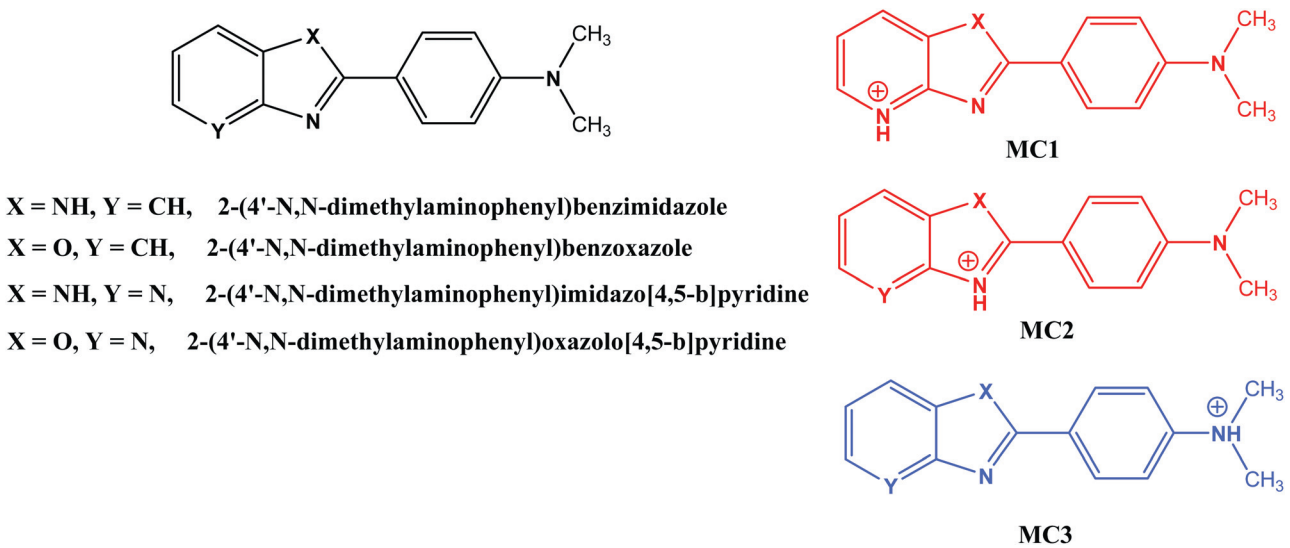

Chart 2 Structures of monocations of DMAPOP and related molecules.

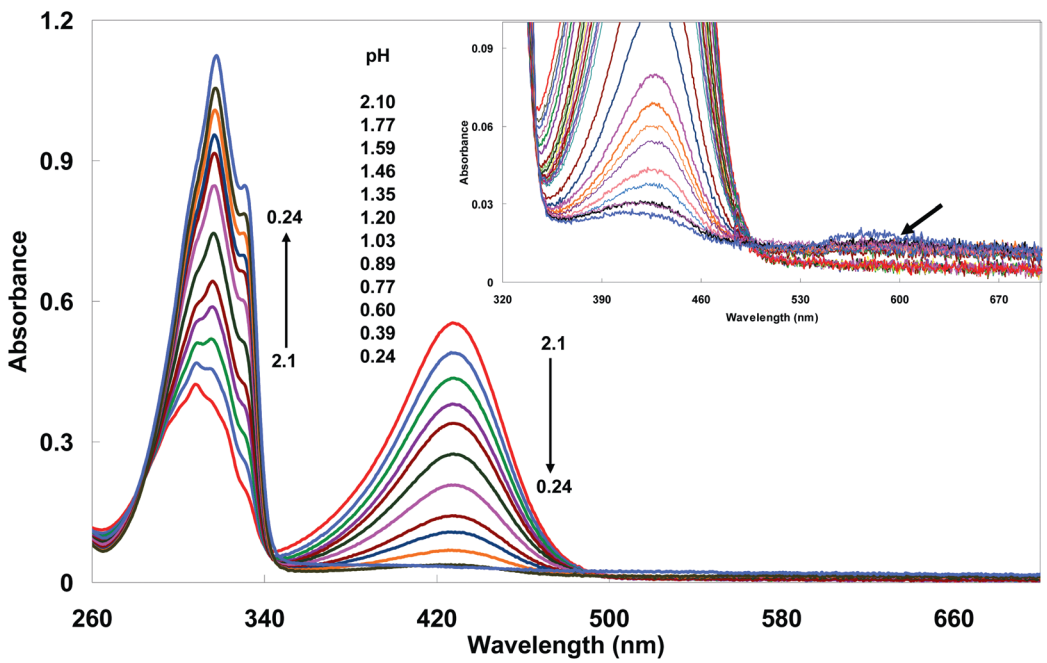

Fig. 8 Absorption spectra of DMAPOP for the monocation(s)-dication(s) equilibrium in water (the insert shows the expanded spectra).

neutral-monocation equilibrium of oxazoles compared to those of imidazoles (Table 3). Since the presence of pyridine nitrogen also decreases the electron density on the oxazole nitrogen, oxazole nitrogen could not be protonated in DMAPOP. This may be due to higher electron density on diethylamino group (over dimethylamino group), as in DEAPOP the protonation at the diethylamino group is higher than that at pyridine nitrogen.[14]

Decreasing the pH of a solution below 2 causes a decrease in the absorbance of MC1 and the absorption spectrum of MC3 also undergoes a bathochromic shift with an increase in absorbance (Fig. 8). At pH 0.18, a clear structured band is observed at 317 nm with a long tail on the red side. These changes are consistent with a shift of the equilibrium towards the dication from the monocation. The absence of an isosbestic point shows the complicated nature of the equilibrium. Three distinct fluorescence spectra were obtained at pH 0.18 while exciting at 316 nm, 428 nm, and 620 nm (Fig. 9). In the absorption spectra of dications, though non-zero absorbance is obtained at around

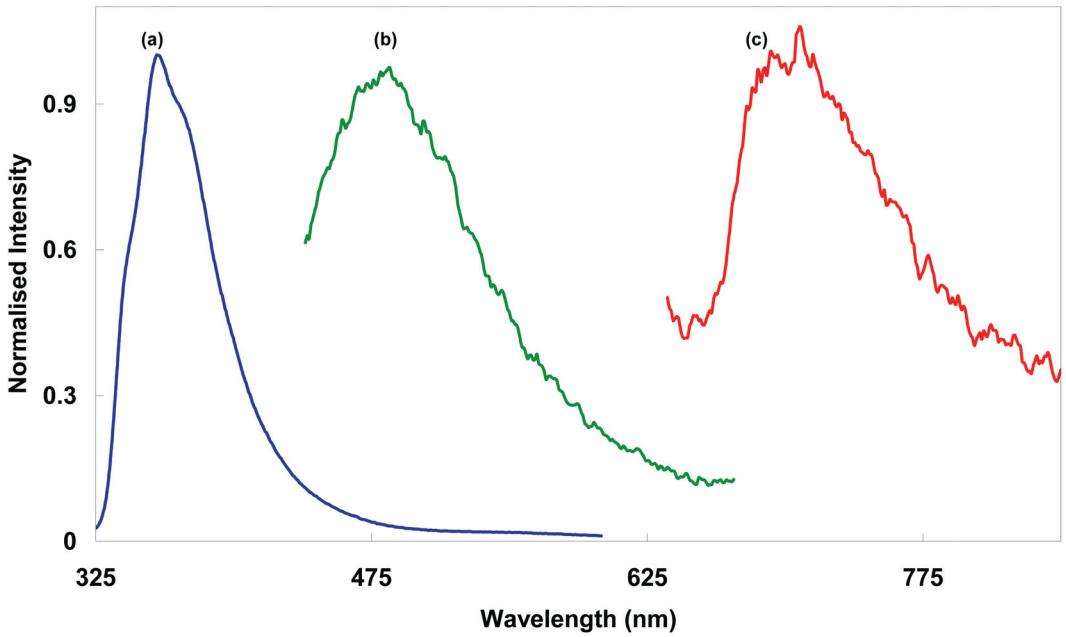

Fig. 9 Normalised emission spectra of DMAPOP for all three dications at pH 0.18: (a) λ_{exc} = 316 nm (DC3), (b) λ_{exc} = 428 nm (DC2), (c) λ_{exc} = 620 nm (DC1).

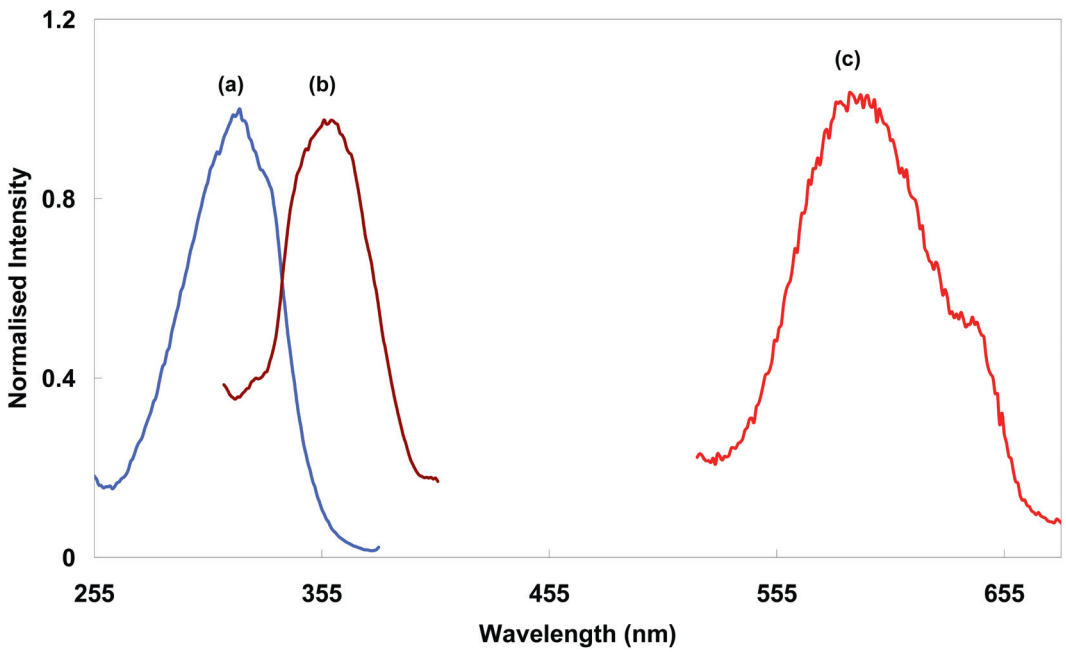

Fig. 10 Normalised excitation spectra of DMAPOP at pH 0.18: (a) λ_{em} = 387 nm (DC3), (b) λ_{em} = 470 nm (DC2), (c) λ_{em} = 710 nm (DC1).

595 nm no clear band is observed. However the excitation spectra recorded clearly shows a band at 595 nm (Fig. 10). The excitation spectra of all the three emission bands at dicationic pH (0.18) are given in Fig. 10. The fluorescence data along with the respective excitation spectral data are compiled in Table 2. The same as the monocations, three types of dications are possible (Scheme 1). A large red shift in the excitation and the emission spectra shows that both the ring nitrogens were protonated; therefore emission band at 702 nm and the corresponding excitation band at 595 nm can be assigned to DC1, which is formed from MC1. The excitation band at 360 nm and the fluorescence band at 480 nm are blue shifted with respect to those of MC1 and red shifted to those of MC3 and these bands can be assigned to DC2 formed by the protonation of both pyridine and dimethylamino nitrogens. The last excitation band at 319 nm and the emission band at 360 nm can be assigned to DC3 and as expected it is red shifted with respect to MC3 and blue shifted compared to MC1 and other dications. The large shift in the emission spectrum of DC1 compared to the other dications may be due to higher charge transfer in DC1, where both protonations occurred at the

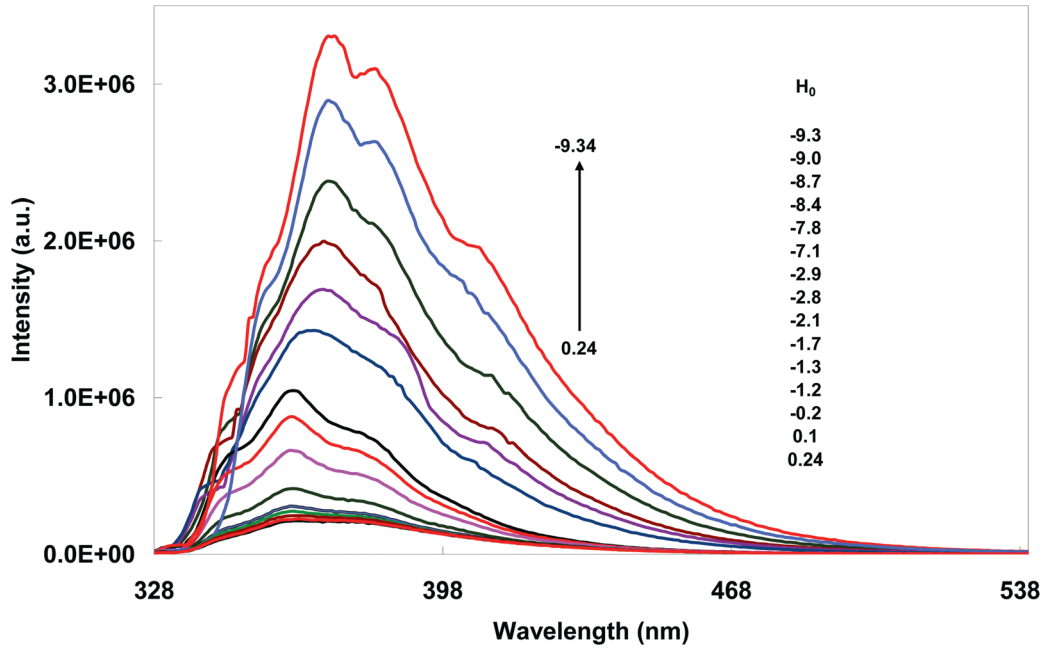

Fig. 11 Emission spectra for dication-trication equilibrium of DMAPOP (λ_{exc} = 318 nm).

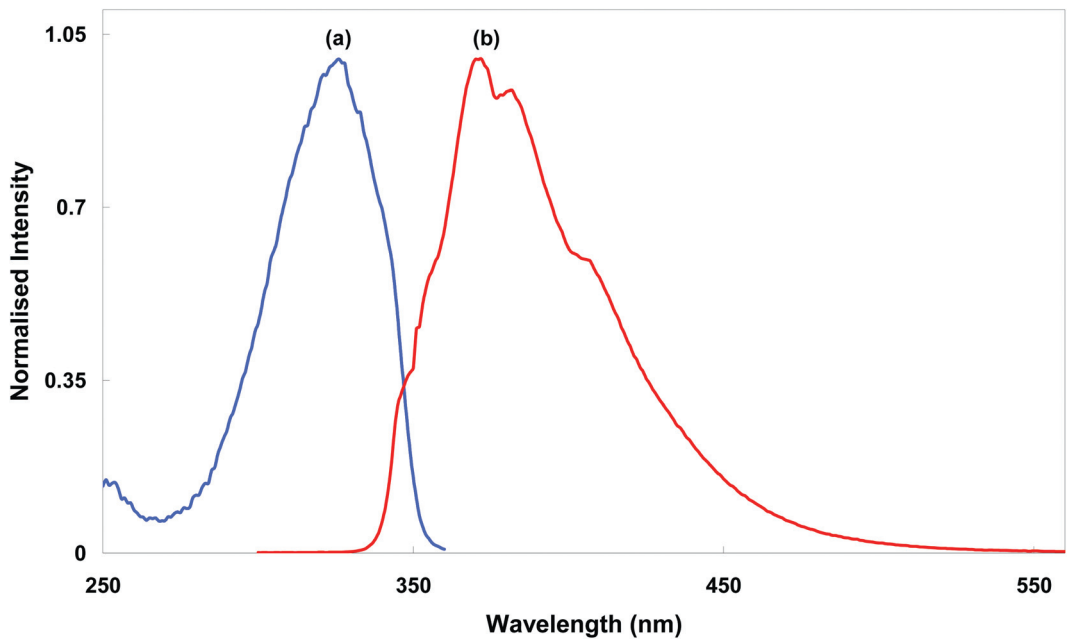

Fig. 12 Normalised excitation and emission spectra of DMAPOP for trication (in conc. H_2SO_4): (a) λ_{em} = 370 nm, (b) λ_{exc} = 320 nm.

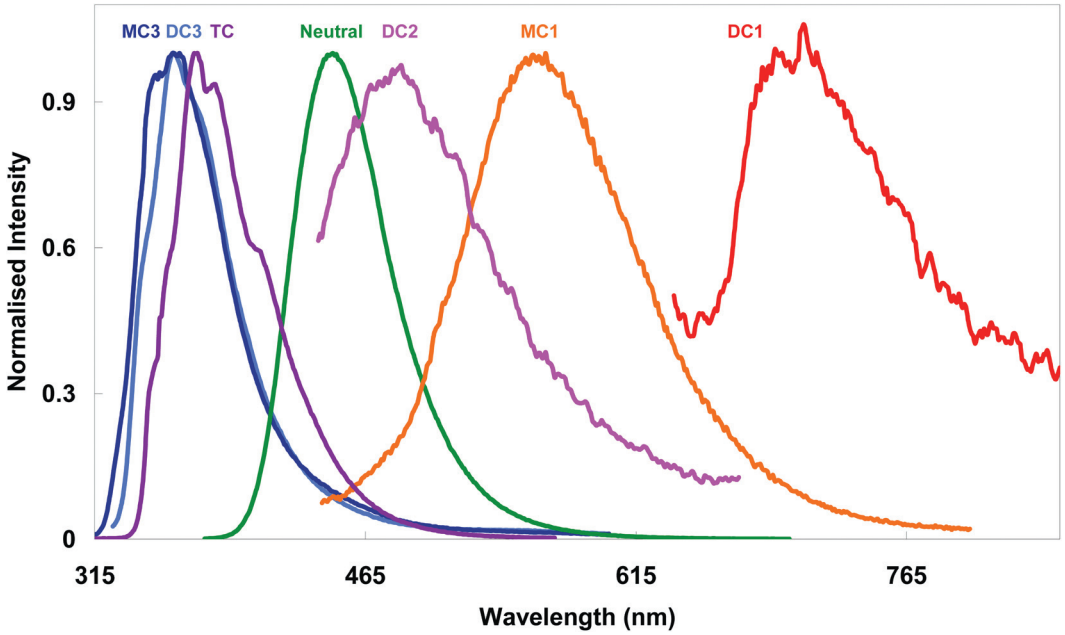

Fig. 13 Normalised emission spectra of DMAPOP for all the prototropic species.

acceptor ring, and, on the other hand, the protonation at dimethylamino nitrogen (donor) will retard the charge transfer in DC2 and DC3.

The fluorescence spectra of DMAPOP at pH lower than 0.18 are shown in Fig. 11. The spectral changes indicate the shifting of equilibrium towards trication. In concentrated sulphuric acid at H_0 −9.4 single excitation and single emission spectra were obtained (Fig. 12). These spectra confirm the formation of trication by protonation of all three nitrogens. For comparison purposes the fluorescence spectra of all the prototropic species of DMAPOP (Scheme 1) are compiled in Fig. 13.

4. Conclusion

The emission characteristics of DMAPOP are significantly different from those of its imidazole analogue DMAPIP in protic solvents. It emits single emission from the intramolecular charge transfer state in both protic and aprotic solvents. No protic induced dual emission is observed in DMAPOP. Further investigations are required to understand the mechanism of dual emission in DMAPIP. Multiparametric regression analysis suggested all three parameters contribute to the stabilization of both ground and excited states. However the relative contribution of dipolar interactions and hydrogen-bond donating ability of the solvent enhanced in the excited state and that of the acceptor ability of solvents is reduced in the excited state. The quantum yield decreases in polar protic solvents due to an increase in the non-radiative rate by hydrogen bonding interactions. DMAPOP also forms two kinds of monocations in the ground and the excited states. But, unlike DMAPIP, monocations are formed by protonation of pyridine and dimethylamino nitrogen. Though the dication equilibrium is dominated by DC3, two other dications DC1 and DC2 also exist in aqueous media.

Acknowledgements

The authors acknowledge department of science and technology (DST), New Delhi for the financial support.

References

1 R. L. Clark, A. A. Pessolano, B. Witzel, T. Lanza, T. Y. Shen, C. G. VanArman and E. A. Risley, 2-(Substituted phenyl)oxazolo[4,5-*b*]-pyridines and 2-(substituted phenyl)oxazolo[5,4-*b*]pyridines as nonacidic antiinflammatory agents, *J. Med. Chem.*, 1978, **21**, 1158–1162.
2 E. Barni, S. Pasquino, P. Savarino, G. D. Modica and G. Giraudo, Disperse and cationic dyes from 2-(o, m, p-Aminophenyl)oxazolo[4,5-*b*]-pyridine, *Dyes Pigm.*, 1985, **6**, 1–12.
3 S. P. G. Costa, E. Oliveira, C. Lodeiro and M. M. M. Raposo, Synthesis, characterization and metal ion detection of novel fluoroionophores based on heterocyclic substituted alanines, *Sensors*, 2007, **7**, 2096–2114.
4 S.-I. Um, Synthesis and biological evaluation of 5-substituted and 4,5-disubstituted-2-arylamino oxazole TRPV1 antagonists, *Dyes Pigm.*, 2007, **75**, 185–188.
5 K. Tanaka, T. Kumagai, H. Aoki, M. Deguchi and S. Iwata, Application of 2-(3,5,6-Trifluoro-2-hydroxy-4-methoxyphenyl)benzoxazole and benzothiazole to fluorescent probes sensing pH and metal cations, *J. Org. Chem.*, 2001, **66**, 7328–7333.
6 J.-P. Fouassier, D.-J. Lougnot, F. Wieder and J. Faure, Laser investigations of some oxazole and oxadiazole derivatives, *J. Photochem.*, 1977, **7**, 17–28.
7 R. J. Perner, J. R. Koenig, S. DiDomenico, A. Gomtsyan, R. G. Schmidt, C.-H. Lee, M. C. Hsu, H. A. McDonald, D. M. Gauvin, S. Joshi, T. M. Turner, R. M. Reilly, P. R. Kym and M. E. Kort, Synthesis and biological evaluation of 5-substituted and 4,5-disubstituted-2-arylamino oxazole TRPV1 antagonists, *Bioorg. Med. Chem.*, 2010, **18**, 4821–4829.
8 R. N. Dsouza, U. Pischel and W. M. Nau, Fluorescent dyes and their supramolecular host/guest complexes with macrocycles in aqueous solution, *Chem. Rev.*, 2011, **111**, 7941–7980.
9 N. Dash, F. A. S. Chipem, R. Swaminathan and G. Krishnamoorthy, Hydrogen bond induced twisted intramolecular charge transfer in 2-(4′-*N*,*N*-dimethylaminophenyl)imidazo[4,5-*b*]pyridine, *Chem. Phys. Lett.*, 2008, **460**, 119–124.
10 G. Krishnamoorthy, *Hydrogen Bonding Effects on Intramolecular Charge Transfer*, ed. K.-L. Han and G. J. Zhao, John Wiley & Sons Ltd., 2011, vol. 1, pp. 313–327.

11 F. A. S. Chipem, A. Mishra and G. Krishnamoorthy, The role of hydrogen bonding in excited state intramolecular charge transfer, *Phys. Chem. Chem. Phys.*, 2012, DOI: 10.1039/c2cp23879a.

12 N. Dash, F. A. S. Chipem and G. Krishnamoorthy, Encapsulation of 2-(4′-*N*,*N*-dimethylaminophenyl)imidazo[4,5-*b*]pyridine in b-cyclodextrin: effect on H-bond-induced intramolecular charge transfer emission, *Photochem. Photobiol. Sci.*, 2009, **8**, 1708–1715.

13 N. Dash and G. Krishnamoorthy, Photophysics of 2-(4′-*N*,*N*-dimethylaminophenyl)imidazo[4,5-*b*]pyridine in Micelles: selective dual fluorescence in sodium dodecylsulphate and triton X-100, *J. Fluoresc.*, 2010, **20**, 135–142.

14 M. Mac, W. Baran, T. Uchacz, B. Baran, M. Suder and S. Lesniewski, Fluorescence properties of the derivatives of oxazolo[4,5-*b*]pyridine, *J. Photochem. Photobiol., A*, 2007, **192**, 188–196.

15 V. Bavetsias, C. Sun, N. Bouloc, J. Reynisson, P. Workman, S. Linardopoulos and M. Edward, Hit generation and exploration: imidazo[4,5-*b*]pyridine derivatives as inhibitors of Aurora kinases, *Bioorg. Med. Chem. Lett.*, 2007, **17**, 6567–6571.

16 M. J. Jorgenson and D. R. Hartter, A critical re-evaluation of the Hammett acidity function at moderate and high acid concentrations of sulphuric acid. New H_0 values based solely on a set of primary aniline indicators, *J. Am. Chem. Soc.*, 1963, **85**, 878–883.

17 A. Crosby and J. N. Demas, Measurement of photoluminescence quantum yields. Rev., *J. Phys. Chem.*, 1971, **75**, 991–1024.

18 M. H. Abraham, P. L. Greillier, J. L. M. Abboud, R. M. Doherty and R. W. Taft, Solvent effects in organic chemistry – recent developments, *Can. J. Chem.*, 1988, **66**, 2673–2686.

19 M. J. Kamlet, J. L. M. Abboud, M. H. Abraham and R. W. Taft, Linear solvation energy relationships. 23. A comprehensive collection of the solvatochromic parameters, π*, α, and β, and some methods for simplifying the generalized solvatochromic equation, *J. Org. Chem.*, 1983, **48**, 2877–2887.

20 C. Reichardt, Empirical parameters of solvent polarity as linear free-energy relationships, *Angew. Chem., Int. Ed. Engl.*, 1979, **18**, 98–110.

21 E. Lippert, Spektroskopische bistimmung des dipolmomentes aromatischer verbindugen im ersten angeregten singulettzustand, *Z. Electrochem.*, 1957, **61**, 962–975.

22 M. J. Frisch, G. W. Trucks, H. B. Schlegel, G. E. Scuseria, M. A. Robb, J. R. Cheeseman, J. A. Montgomery, Jr., T. Vreven, K. N. Kudin, J. C. Burant, J. M. Millam, S. S. Iyengar, J. Tomasi, V. Barone, B. Mennucci, M. Cossi, G. Scalmani, N. Rega, G. A. Petersson, H. Nakatsuji, M. Hada, M. Ehara, K. Toyota, R. Fukuda, J. Hasegawa, M. Ishida, T. Nakajima, Y. Honda, O. Kitao, H. Nakai, M. Klene, X. Li, J. E. Knox, H. P. Hratchian, J. B. Cross, V. Bakken, C. Adamo, J. Jaramillo, R. Gomperts, R. E. Stratmann, O. Yazyev, A. J. Austin, R. Cammi, C. Pomelli, J. W. Ochterski, P. Y. Ayala, K. Morokuma, G. A. Voth, P. Salvador, J. J. Dannenberg, V. G. Zakrzewski, S. Dapprich, A. D. Daniels, M. C. Strain, O. Farkas, D. K. Malick, A. D. Rabuck, K. Raghavachari, J. B. Foresman, J. V. Ortiz, Q. Cui, A. G. Baboul, S. Clifford, J. Cioslowski, B. B. Stefanov, G. Liu, A. Liashenko, P. Piskorz, I. Komaromi, R. L. Martin, D. J. Fox, T. Keith, M. A. Al-Laham, C. Y. Peng, A. Nanayakkara, M. Challacombe, P. M. W. Gill, B. Johnson, W. Chen, M. W. Wong, C. Gonzalez and J. A. Pople, *Gaussian 03 (Revision E.01)*, Gaussian, Inc., Wallingford, CT, 2004.

23 S. Dhar, D. K. Rana, S. S. Roy, S. Roy, S. Bhattacharya and S. C. Bhattacharya, Effect of solvent environment on the photophysics of a newly synthesized bioactive 7-oxy(5-selenocyanato-pentyl)-2*H*-1-benzopyran-2-one, *J. Lumin.*, 2012, **132**, 957–964.

24 Y. Kim, M. Yoon and D. Kim, Excited-state intramolecular proton transfer coupled-charge transfer of *p*-*N*,*N*-dimethylaminosalicylic acid in aqueous β-cyclodextrin solutions, *J. Photochem. Photobiol., A*, 2001, **138**, 167–175.

25 G. Krishnamoorthy and S. K. Dogra, Spectral characteristics of various prototropic species of 2-(4′-*N*,*N*-dimethylaminophenyl)pyrido[3,4-*d*]imidazole, *J. Org. Chem.*, 1999, **64**, 6566–6574.

26 J. K. Dey and S. K. Dogra, Dual fluorescence of 2-(4′-*N*,*N*-(dimethylamino)phenyl)benzothiazole and its benzimidazole analogue: effects of solvents and pH on electronic spectra, *J. Phys. Chem.*, 1994, **98**, 3638–3644.

27 N. Dash, F. A. S. Chipem and G. Krishnamoothy, Encapsulation of 2-(4′-*N*,*N*-dimethylamino)-phenylimidazo[4,5-*b*]pyridine in β-cyclodextrin: effect on H-bond-induced intramolecular charge transfer emission, *Photochem. Photobiol. Sci.*, 2009, **8**, 1708–1715.

28 G. Krishnamoorthy and S. K. Dogra, Dual fluorescence of 2-(4′-*N*,*N*-dimethylaminophenyl)benzoxazole, *Chem. Phys.*, 1999, **243**, 45–59.

29 G. Krishnamoorthy and S. K. Dogra, Dual fluorescence of 2-(4′-*N*,*N*-dimethylaminophenyl)benzimidazole: effect of β-cyclodextrin and pH, *J. Photochem. Photobiol., A*, 1999, **121**, 109–119.

